Indian Journal of Engineering & Materials Sciences
Vol. 11, December 2004, pp. 465-472

An investigation on the applicability of Cartesian grid approach to calculate flow over arbitrary terrain

S Vengadesan[a*], A Nakayama[b] & S Yokojima[c]

[a]Department of Applied Mechanics, Indian Institute of Technology, Chennai 600 036, India

[b]Department of Science of Regional and Built Environments, Graduate School of Science and Technology
Kobe University, Kobe 657 8501, Japan

[c]Enviornmental Fluid Mechanics Laboratory, Department of Civil and Environmental Engineering
Stanford University, Stanford, CA 94395-4020, USA

Received 17 December 2003; accepted 9 September 2004

An investigation is made on the applicability of method of representing by Cartesian grid to calculate flow over natural terrain. Model hill geometry with different maximum slope angles is chosen and calculations by both Cartesian and Boundary-fitted coordinate representations are made. Computations are performed for laminar flow at different Reynolds numbers and turbulent flow conditions. Results in terms of mean velocity distribution, streamline, vorticity distribution and velocity vector close to the surface are analyzed and discussed. The study indicates that to calculate flow over undulating natural terrain, rectangular coordinate method of representing the geometry is able to capture most of the flow phenomena and it can be a viable alternative.

IPC Code: Int Cl.[7] G01F 1/00, F15D

Increasing power of computers and recent advancements in numerical methods have made computational fluid dynamics (CFD) as a powerful tool to calculate and predict flows of various kinds. Application of CFD technique to calculate complex three-dimensional flows in natural environment is becoming possible. One of the main difficulties in atmospheric applications is to represent undulating natural topography. Conventional method to deal with curved boundary is to use coordinate system that fits the boundary curves. Once a good grid is generated, boundary conditions are set at exact locations and the flow over it can be calculated with relative ease. For more complex boundaries, finite element methods or finite difference methods on unstructured grids are considered promising and many efforts are made in this direction. However, when the boundary becomes irregular or not smooth, it becomes impossible to generate a grid. In such a situation, usually, one has to resort to other methods like a multi-block approach or local refinement, but generating a grid with good quality becomes difficult. Furthermore, transformation of the governing equations results in a complex system of equations with many geometric parameters implying high computational overhead. So, some kind of approximation is necessary and a classical method of using simple rectangular Cartesian coordinates may be seen as an alternative choice.

In Cartesian method, generation of grid is trivial and arbitrary shapes can be represented. Because of this advantage, many new methods of using rectangular grids for complex shapes with various boundary treatments are proposed[1,2]. Many researchers have adopted Cartesian coordinate method[3-6]. However, all these methods require geometry definition, and they are not available for natural terrain or any undulating geometry. One disadvantage of using the rectangular grid for an arbitrary shape is that either the position of the boundary becomes approximate or the boundary conditions are applied at interpolated points. In computing flows over complex topography or similar complex boundary, it will help if relative performance and accuracies are known for these different methods of representing the geometry in context with both overall results and behaviour of different differencing schemes used to discretize the non-linear convective terms.

In the present work, test case of flow over smooth curved hill is considered and calculation using both boundary-fitted coordinates and the Cartesian coordinates are compared. First, basic performance of each method is examined in low-Reynolds number

*For correspondence: (E-mail: vengades@iitm.ac.in)

laminar flow, and then accuracies and stability are examined at high Reynolds numbers. Then the methods are evaluated when applied to large-eddy simulation (LES) of higher Reynolds number turbulent flow in the same geometrical region. The test calculations for the turbulent case are performed for the cases in which detailed experimental data are available.

Numerical Strategy for Rectangular Grid (RC)

Here, the numerical methods adopted while using the rectangular grid are described. They are for computing the flow of incompressible fluid of density ρ and kinematic viscosity ν. The governing equations are the conservation equations for mass and momentum

$$\frac{\partial u_i}{\partial x_i} = 0 \qquad \ldots (1)$$

$$\frac{\partial u_i}{\partial t} + u_j \frac{\partial u_i}{\partial x_j} = -\frac{1}{\rho}\frac{\partial p}{\partial x_i} + \nu \frac{\partial^2 u_i}{\partial x_j \partial x_j} \qquad \ldots (2)$$

Here u_i is the component of the velocity vector in the Cartesian coordinate x_i. We also use the notation (x,y,z) for (x_1,x_2,x_3) and (u,v,w) for (u_1,u_2,u_3). These equations are discretized, with variables arranged in staggered system to apply conveniently the pressure-coupling algorithm. Figure 1 shows the grid arrangement and the points where the boundary conditions are applied when the same scheme is used for an arbitrary geometry. Discretization of convective terms are done by a third-order upwind differencing-UTOPIA, or by conservative second-order central difference scheme[7]. Viscous terms are discretized by second-order accurate central differencing scheme. HSMAC iteration procedure is used for calculating pressure. Time advancing of the momentum equations is done by a second-order accurate explicit, Adams-Bashforth method. Performance of the code with numerical strategy for RC has been validated for laminar and turbulent flow past a square cylinder against available numerical and experimental results[8].

Numerical Strategy for Boundary-Fitted Grid (BFC)

In order to solve the same incompressible flows in boundary-fitted grid, Eqs (1) and (2) are transformed in general coordinates and they are given as:

$$\frac{\partial U_m}{\partial \xi_m} = 0 \qquad \ldots (3)$$

$$J^{-1}\frac{\partial u_i}{\partial t} + \frac{\partial}{\partial \xi_m}\{U_m u_i\} = -\frac{\partial}{\partial \xi_m}\left\{A_i^m \frac{p}{\rho} - \nu G^{mn}\frac{\partial u_i}{\partial \xi_n} - \nu J^{-1}\frac{\partial \xi_m}{\partial x_j}\frac{\partial \xi_n}{\partial x_i}\frac{\partial u_j}{\partial \xi_n}\right\} \qquad \ldots (4)$$

where

$$J^{-1} = \det\left(\frac{\partial x_i}{\partial \xi_j}\right); \quad A_i^m = J^{-1}\frac{\partial \xi_m}{\partial x_i}; \quad G^{mn} = J^{-1}\frac{\partial \xi_m}{\partial x_j}\frac{\partial \xi_n}{\partial x_j}; \quad U_m = A_m^j u_j. \qquad \ldots (5)$$

Here, x_i is the Cartesian coordinate fixed in the physical space and ξ_m is the general coordinate used in the computation. J is the Jacobian of the transformation matrix from x_i to ξ_m and U_m is the contravariant component of the velocity vector multiplied by J^{-1}, which represents the volume flux in the direction perpendicular to the surface ξ_m = constant. For laminar flow, the last term will disappear and for turbulent flow, which is solved assuming the eddy-viscosity formulation for the sub-grid scale stresses, the eddy viscosity ν_G is added to ν as explained in the next section.

The staggered grid is an effective method of avoiding the pressure oscillation, but it is not suited for the general coordinates. The control volumes in which conservation laws are applied are different for different components of momentum and the codes become excessively complex for three-dimensional cases with many elements of the metric tensor required to be stored. This results in complex coding and additional computational loads. Recently,

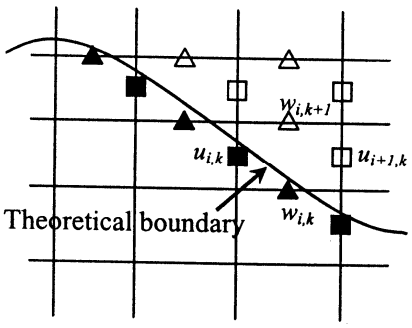

Fig.1—Grid arrangement; boundary conditions are enforced at locations marked by filled symbols

collocated grid arrangement, in which the velocity components and the pressure are defined at the cell center and the fluxes are defined on the cell-bounding surfaces, has been proposed and found to be effective[9]. Therefore, the method based on the collocated variables is used here. Figure 2 shows the collocated grid arrangement of variables adopted in the present work. In the collocated grid, the basic variables u_i and p are defined at the cell center and the differencing of the conservations of equations of momentum is done the same way as in the case of regular grid, while differencing of the conservation of mass is done using the volume flux U_i, defined at the center of the cell surface so that pressure oscillation is controlled the same way as the staggered grid methods. The method, we take is very close to that of Zang *et al.*[9] and follow the fractional-step method with the Crank-Nicolson implicit differencing for the diagonal elements of the viscous terms and the second-order Adams-Bashforth scheme for the off-diagonal viscous terms and the advective terms. The accuracy of interpolation for the volume fluxes on the cell surfaces needed in the collocated grid is improved by using the method of Inagaki and Abe[10]. The spatial differencing of the nonlinear advective terms is done by either the second-order conservative scheme or UTOPIA. All other spatial differencings are done by the second-order central differencing scheme.

The above-described methods incorporating numerical strategy for Boundary-fitted coordinate representation have been coded and performance of the code with numerical strategy for BFC has been validated against laminar flow in a curved cavity laminar, an external flow above a curved hill and DNS of fully-developed flow in a two-dimensional open channel[11].

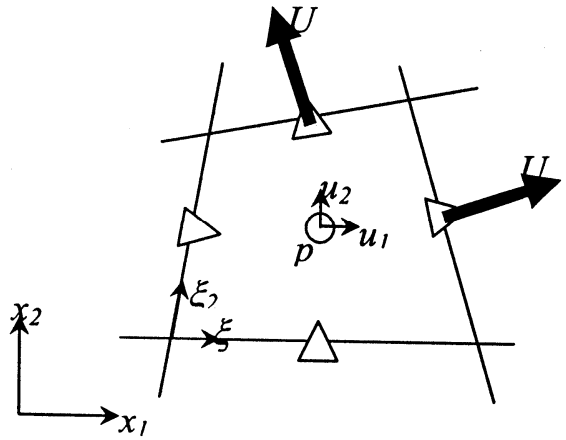

Fig. 2—Variables in collocated arrangement

Sub-grid Stress Model for LES

When the above methods of flow solution are used in large eddy simulation (LES) of turbulent flows, all variables in the equations are the respective filtered quantities of the instantaneous flow. The additional stress called subgrid-scale stress R_{ij} appears in the momentum equations. If it is modeled by conventional eddy-viscosity model, which is given as,

$$R_{ij} = \frac{2}{3} k_s \delta_{ij} - 2\nu_G S_{ij} \quad \ldots (6)$$

where, k_s is the sub-grid turbulent kinetic energy, δ_{ij} is the Kronecker delta, ν_G is the sub-grid eddy viscosity and S_{ij} is the strain tensor, then ν_G needs to be added ν in the momentum equations. ν_G is modeled by the Smagorinsky model

$$\nu_G = (C_S \Delta)^2 \left[\frac{\partial u_i}{\partial x_j} \left(\frac{\partial u_i}{\partial x_j} + \frac{\partial u_j}{\partial x_i} \right) \right]^{1/2} \quad \ldots (7)$$

where, Δ is the grid size defined by the geometric average of the grid spacings in three directions, $(\Delta x_1 \Delta x_2 \Delta x_3)^{1/3}$, u_i is now the spatially filtered velocity. C_S is Smagorinsky constant, which is chosen as 0.13. In the case of BFC, coordinate transformed equations of (6) and (7) are used.

Test Flow Past a Model Curved Hill

The flow configuration considered shown in Fig. 6 is that past a model isolated hill. It is a smooth two-dimensional topography, defined by an analytical expression $\frac{z_G}{H} = \frac{1}{1+(x/nH)^4}$, where z_G is the elevation of the ground at horizontal position x, and H is the height of the hill and x is the horizontal distance from the center of the hill. Reynolds number Re for the present flow configuration is defined by the oncoming velocity U_{ref} and maximum hill height H. The steepness of the hill is determined by the value of n. For n=2.8, the largest slope angle is 20 degrees and the flow in this case contains a small separate bubble at low Reynolds numbers. For n=2.3, the largest slope is 25 degrees and the flow is considerably different with larger flow separation. For n=2.0, the largest slope is 15 degrees. These are the test cases used for the present comparative test runs. Calculations are performed at two Reynolds numbers of 100 and 500

and results at Re=100 are compared with available numerical results[12].

Computational Domain and Grid

The computational region covers the test flow shown in Fig. 3. In RC, the geometry is approximated and the boundary condition is applied at the grid point nearest to the theoretical boundary. The computational domain extends from about 8.5H upstream and 14H downstream of the hill of 25 degrees. For the hill with maximum slope angle of 20 degrees, it covers the region from -10.5H to 17H. The calculation domain extends 7H in the cross-stream-wise and 4H in the span-wise directions. In the stream-wise direction, points are closely spaced within 4H on either side from the hill summit. In the cross-stream-wise direction, the first point from the ground is placed at 0.03H near the bottom of the wall, stretched up to 0.5H and then compressed up to 1.2H and then placed non-uniformly until the top boundary. In the span-wise direction in either grid system, grids are uniformly spaced. The total grid size is 128×21×61 and 140×21×61 respectively for 25-degree and 20-degree slope hills. The computational domain for hill with maximum slope angle of 15 degrees covers the region of 12H and 19H on the upstream and downstream respectively. In the other directions, the domain is kept the same as that used for 25 degrees case. The total grid size used is 141×21×61.

In the case of BFC, the grid is generated by transforming the physical space on the rectangular computational space by an elliptic equation and generated coordinates fit the actual boundary. The mesh is made orthogonal near the boundary since in that situation, boundary condition for pressure is not required, if staggered or collocated grid is used. In order to compare the results with those by RC, calculation domain, distance of the first grid point from the ground and grid size is the kept as that of in RC. Fig. 4 shows the typical computational grid used for hill with maximum slope angle of 20 degrees.

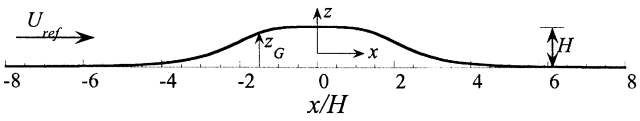

Fig. 3—Geometry of flow over a curved hill

Boundary Conditions

Boundary conditions are enforced at inflow, downstream, top and bottom boundaries. Periodic boundary conditions are enforced for the span-wise direction. Non-slip boundary conditions are applied on the ground surface and slip conditions on the top boundary. At the downstream plane, the radiation boundary conditions are used. At the inflow plane, uniform flow is specified for low Reynolds number test cases.

Results and Discussion

Calculations at low Reynolds number flow

Table 1 gives the list of calculation cases and keys used for laminar flow calculation. Calculations are run with non-dimensional time increment of Δt=0.001H/U_{ref} and the results are compared at the same non-dimensional time T=40H/U_{ref}. In order to assess the numerical methods with UTOPIA scheme, which is known to introduce numerical viscosity and conservative central scheme, calculations are performed for the hill with maximum slope angle of 20 degrees at Re=100, and compared with numerical calculation. Figure 5a presents a comparison of streamlines, and good agreement is seen. Contours of transverse vorticity obtained by RC and present BFC grids are compared in Fig. 5b with those by Miyashita[12]. In Ref.12, calculation is two-dimensional

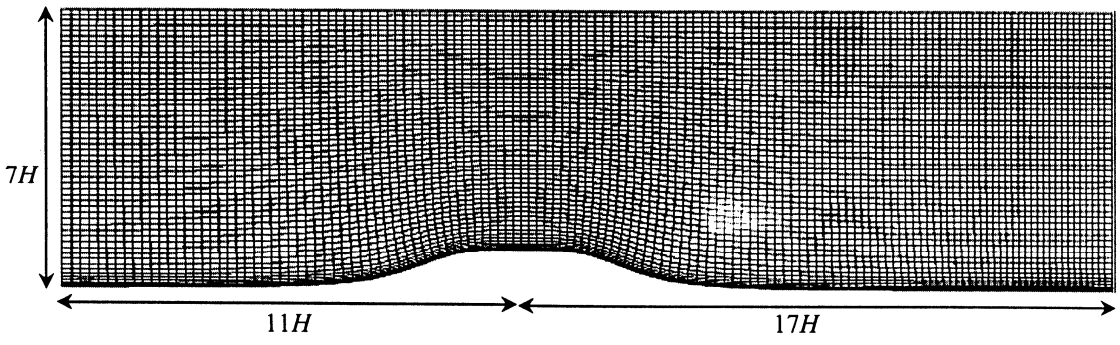

Fig. 4—BFC grid used for flow over model hill geometry

Table 1—Details of calculation cases

Maximum slope angle	*Re*	Grid arrangement	Scheme	Key used
20	100	RC	conservative central (CC2)	H201RC
		RC	upwind (UB3)	H201RU
		BFC	conservative central	H201BC
		BFC	upwind	H201BU
25	100	RC	conservative central	H251R
		BFC	conservative central	H251B
		RC	conservative central	H255R
	500	BFC	conservative central	H255B
	13000	RC	upwind	-
		BFC	upwind	-
15	13000	RC	upwind	-
		BFC	upwind	-

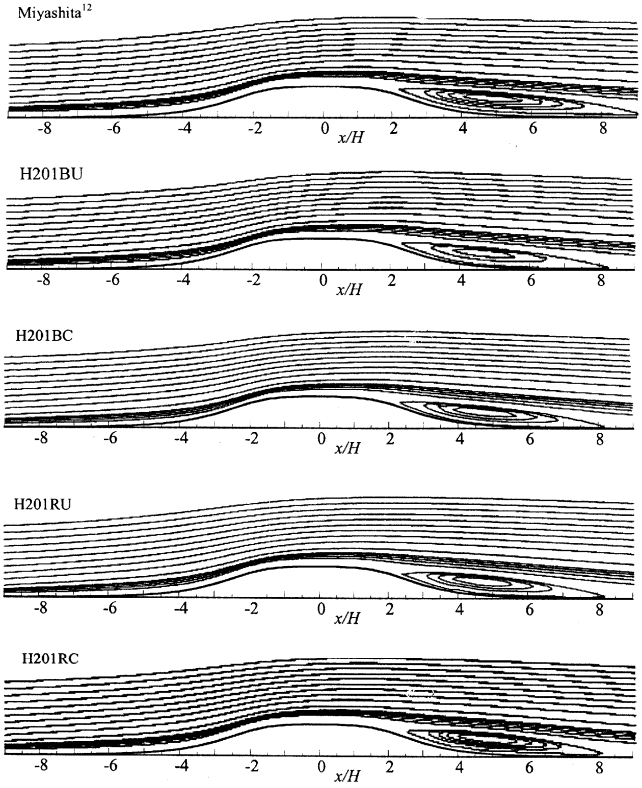

(a) streamlines

Fig. 5a—Comparison of calculation results for hill with maximum slope angle of 20 degrees streamlines

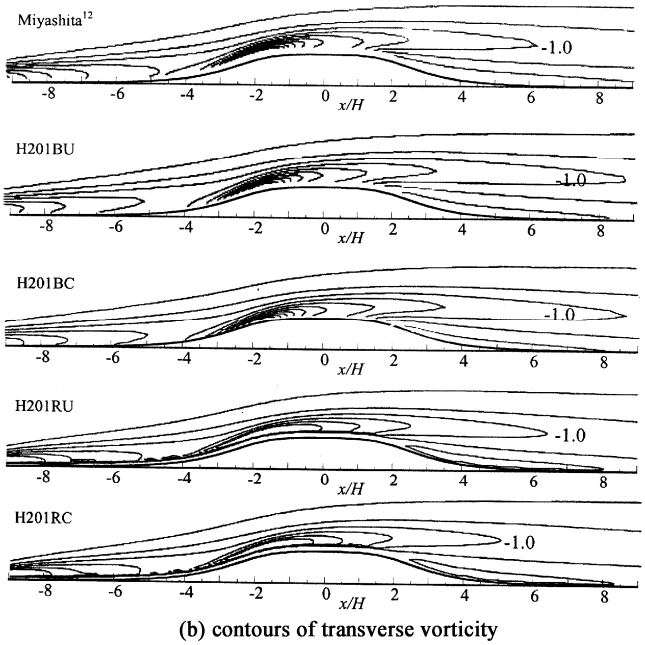

(b) contours of transverse vorticity

Fig. 5b—Comparison of calculation results for hill with maximum slope angle of 20 degrees contours of transverse vorticity

and numerical methods adopted in that study to perform URANS calculations are reported in Nakayama and Miyashita[13]. Much denser grid of 260×70 is used and the numerical accuracy is considered to be better. Results agree very well although the recirculation flow is calculated slightly weaker in both RC and BFC. Figure 5c presents a comparison of the profiles of stream-wise velocity component u/U_{ref} by RC and BFC along several stream-wise stations. Small difference between results by upwind and central scheme in RC is noticed. But, the agreement is generally good as expected from the comparison of the streamlines. These mean that RC and BFC calculations with an appropriate upwind scheme and conservative central scheme produce good results, comparable with each other and thus the computational methods may be said to have been verified.

Laminar calculations are then performed by both RC and BFC for flow past the hill of maximum slope angle of 25 degrees at low Reynolds number of 100 in order to verify again the basic numerical procedures. Then calculations at higher Reynolds number of 500

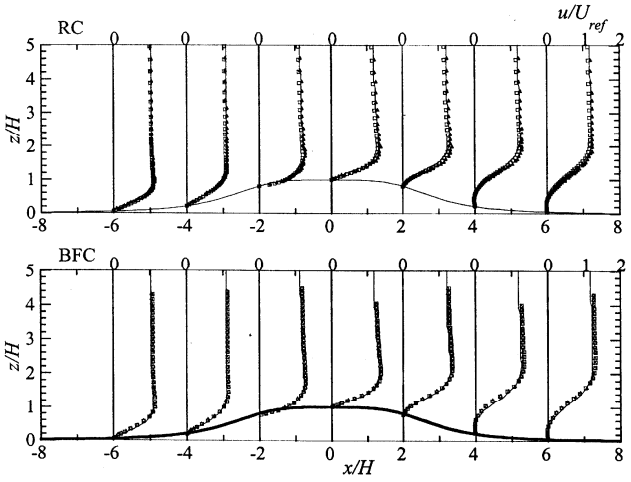

(c) streamwise velocity along specified stations: line – Miyashita[12]; open square – UB3; open triangle – CC2

Fig. 5c—Comparison of calculation results for hill with maximum slope angle of 20 degrees stream-wise velocity along specified stations [(–) Miyashita[12], (□) UB3, (Δ) CC2

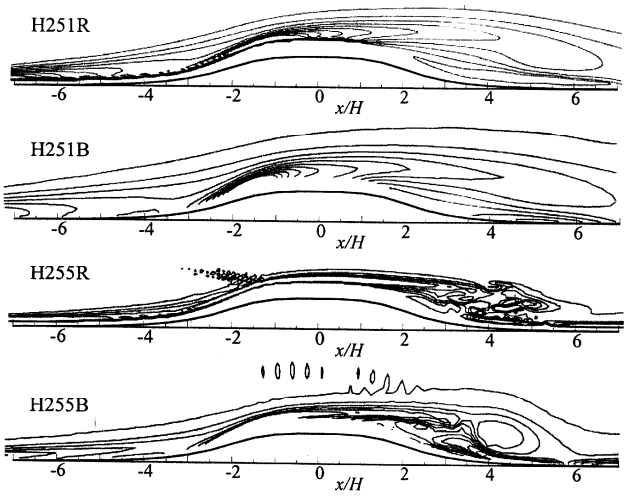

(a) contours of transverse vorticity

Fig. 6a—Comparison of calculation results for hill with maximum slope angle of 25 degrees contours of transverse vorticity

are performed. The calculated span-wise vorticity distribution and streamlines by RC and BFC are shown in Fig. 6. At low *Re*=100, results calculated by both grid systems for all the cases agree well with each other. For higher Reynolds number of 500, we see differences in the calculated results. Small oscillations appear in the plot of span-wise vorticity calculated by RC grid, as noticed while performing calculation of flow past square cylinder[8]. It has also been pointed out Piomelli and Balaras[5] in the calculation of flow past a bluff body similar oscillation appears, when the cell Reynolds number

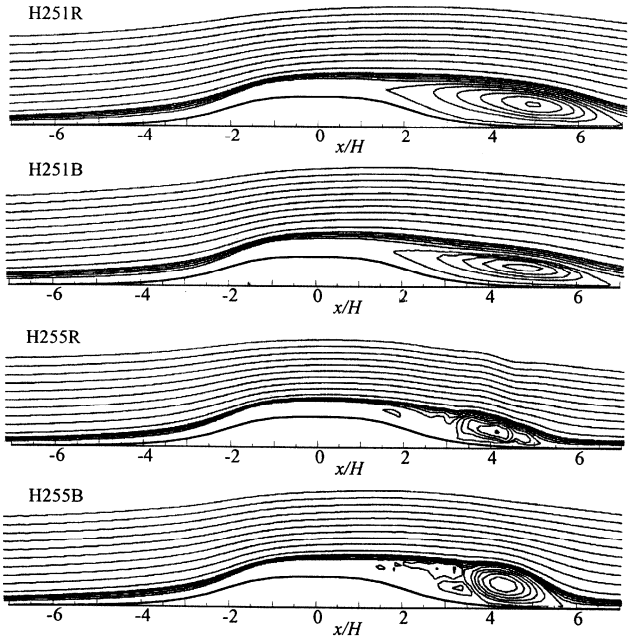

(b) streamline

Fig. 6b—Comparison of calculation results for hill with maximum slope angle of 25 degrees streamline

becomes large and the central differencing is used for convective terms. This phenomenon can be suppressed by using an upwind differencing which appears to be necessary for stable calculation of turbulent flows at much higher Reynolds numbers when performed on Cartesian coordinates.

The results of these laminar flow calculations performed for flow over curved body with unfixed separation with either small separation or large separation by two different coordinate representations of the geometry can be summarized as follows. Basic numerical methods employing conservative central scheme and upwind scheme for convective terms are validated for both BFC and RC for the case of the model hill geometry with maximum slope angle of 20 degrees. At low Reynolds number for this test case, flow experiences small separation, and results by the both schemes on both coordinate representation yield closer results. At higher slope angle and at slightly higher *Re*, while the calculation using the central difference scheme for the convective terms leads to pressure oscillation when the geometry is approximated by rectangular grid, results are stable when the geometry is represented by a boundary-fitted grid or by using upwind scheme.

Calculations at high Reynolds number flow

Comparison for low and moderate Reynolds number flow was discussed. The same investigation is

now extended to high Reynolds number flow. For the same model hill geometry, mean velocity and turbulent stresses have been measured for the Reynolds number based on the oncoming reference velocity U_{ref} and H of 13000 (ref. 14). Model hills of 25 degrees and 15 degrees are considered. LES methodology is adopted. Computation domain, mesh size, and distance of the first grid point were kept same those were used in rectangular coordinate calculation. This grid distribution for the test Reynolds number of 13000 gives vertical distance in viscous units, $z^+=zu_\tau/\nu$ of the first node about 20 and 15 on the top of hill and at x/H=4 respectively for the hill model with maximum slope of 25 degrees and thus viscous layer are not resolved. So, the mesh is not of high resolution to resolve the laminar sub-layer, a key problem encountered in LES of high Reynolds number practical flows when performed with there is a limitation on computer resource. Inflow condition for velocity at station x/H=-4 and x/H=-6 for 25 degrees and 15 degrees respectively are taken from that of experiment. Calculations are made with third-order upwind-biased scheme for convective terms, and non-slip condition as wall boundary condition.

Calculated velocity vectors close to the boundary by both grid systems in the region where the boundary curvature is the largest is presented in Fig. 7 for both hill with 15 degrees and 25 degrees slope angle. This figure shows that there is no such thing as step corners due to the approximation in the rectangular grid. In both cases, vectors are seen to be close to tangent to local boundary. Small deviation of the

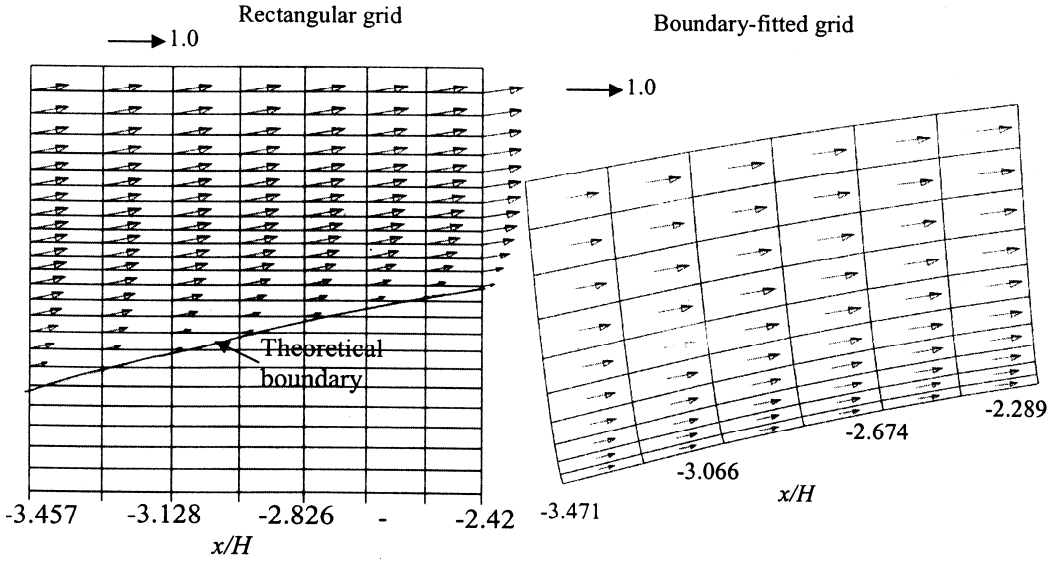

(a) Hill with maximum slope angle of 15 degrees

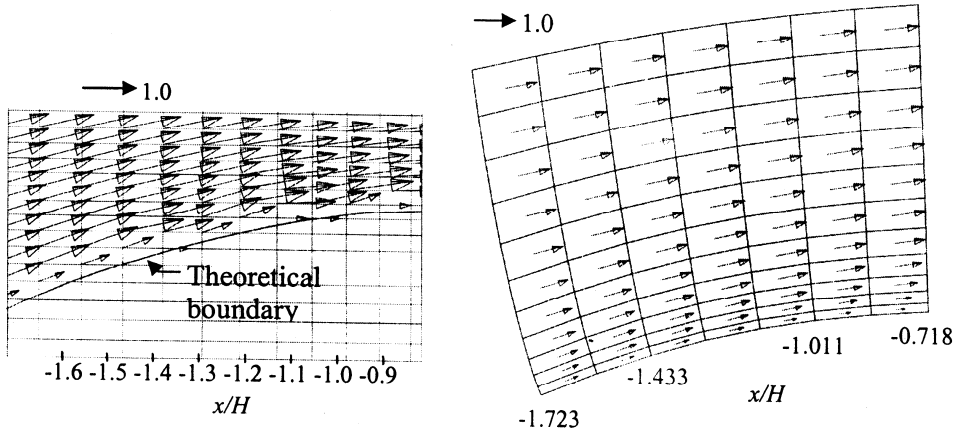

(b) Hill with maximum slope angle of 25 degrees

Fig. 7—Comparison of velocity vector near the solid boundary

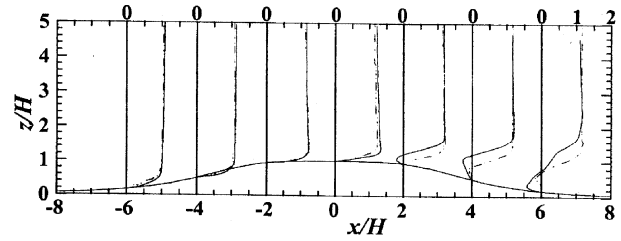

(a) Hill with maximum slope angle of 15 degrees; continuous line: Rectangular grid; chain line – Boundary-fitted grid

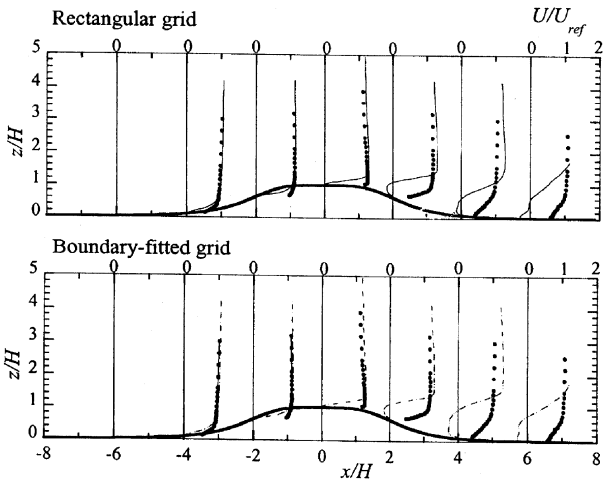

(b) Hill with maximum slope angle of 25 degrees; symbols – Expt.

Fig. 8—Comparison of mean stream-wise velocity (U/U_{ref})

vectors from the direction tangent to the boundary is observed in the case of calculation by rectangular grid. However, this does not influence the results on the whole, with respect to this particular study is concerned, as seen in the results of the mean stream-wise velocity (U/U_{ref}), along specified stream-wise stations shown in Fig. 8. In both test cases of the hill, both geometry representations predict separation, re-circulation and they are qualitatively close to each other.

Conclusions

Flow past model hill geometry is computed by both rectangular and boundary-fitted coordinate representation to investigate the applicability of rectangular coordinate method to calculate flow over natural terrain. Calculations are performed at low and high Reynolds number laminar flows to validate the numerical methods. While the calculation using central difference scheme for the convective terms leads to pressure oscillation when the geometry is approximated by rectangular grid, results are stable when the geometry is represented by a boundary-fitted grid or by using upwind scheme. At higher *Re* for turbulent flow condition, LES calculations results by with UTOPIA scheme for the convective terms show similar trend in both grid systems. Hence, when calculation of flow past natural topography or complex geometry or open-channel flows with deforming free surfaces or flow domain for which it is difficult to generate BFC, is to be performed, rectangular coordinate approximation of the geometry with stability assured by upwind scheme for the convective terms is a good alternative and simulation by this method captures the flow features.

References

1 Forrer H & Jeltch R, *J Comp Phys*, 140 (1998) 259.

2 Goldstein D, Handler R & Sirovich L, *J Comp Phys*, 105 (1993) 354.

3 Ye T, Mittal R, Udayakumar H S & Shyy W, *J Comp Phys*, 156 (1999) 209.

4 Verzicco R, Mohd Yusof J, Orlandi P & Haworth D, *AIAA J*, 38 (2000) 427.

5 Piomelli U & Balaras E, 3rd AFOSR *Int Conf on DNS and LES*, Dallas, USA, 2001, 27.

6 Majumdar S, Iaccarino G & Durbin P, *Annual Research Briefs*, Centre for Turbulence Research, Stanford University, 2001, 353.

7 Morinishi S, Lund T, Vasilyev O V & Moin P, *J Comp Phys*, 143 (1998) 90.

8 Nakayama A & Vengadesan S N, *Int J Numer Methods Fluids*, 38 (2002) 227.

9 Zang Y, Street R L & Koseff J R, *J Comp Phys*, 114 (1994) 18.

10 Inagaki M & Abe K, *Trans JSME B*, 64 (1998) 1981.

11 Vengadesan S, Yokojima S & Nakayama A, *J Aero Soc India*, (2003) (communicated).

12 Miyashita K, Ph.D Thesis, Kobe University, Japan, (2001).

13 Nakayama A & Miyashita K, *Int J Numer Methods Heat Fluid Flow*, 11 (2001) 723.

14 Nakayama A & Yokota D, *Ann J Hydraul Eng, JSCE,* 45 (2001) 43.